

Selected Papers from the 23rd International Radiocarbon Conference, Trondheim, Norway, 17–22 June, 2018
© 2019 by the Arizona Board of Regents on behalf of the University of Arizona. This is an Open Access article, distributed under the terms of the Creative Commons Attribution licence (<http://creativecommons.org/licenses/by/4.0/>), which permits unrestricted re-use, distribution, and reproduction in any medium, provided the original work is properly cited.

ABSOLUTE DATING OF EARLY IRON OBJECTS FROM THE ANCIENT ORIENT: RADIOCARBON DATING OF LURISTAN IRON MASK SWORDS

C Matthias Hüls^{1*}  · Ingo Petri² · Helmut Föll³

¹Leibniz-Laboratory for Radiometric Dating and Isotope Research, Christian-Albrechts-Universität Kiel, Max-Eyth-Str.11-13, 24118, Kiel, Germany

²Institute for Pre- and Protohistoric Archaeology, Christian-Albrechts-Universität Kiel, Kiel, Germany

³Institute for Material Science, Christian-Albrechts-Universität Kiel, Kiel, Germany

ABSTRACT. Luristan Iron Mask Swords have been recovered mostly from illegal diggings in the 1920s. The about 90 known objects are characterized by a disk-shaped pommel on the top of the handle with two mounted bearded heads on two sides. According to the similarity in form and radiocarbon (¹⁴C) measurements on two swords from museum collections, an overall short production period was assumed around 1000 BC (Moorey 1991; Rehder 1991). Here we present the results of metallurgical analysis and ¹⁴C measurements for three newly acquired Luristan swords, which were donated to the Royal Museums of Art & History, Brussels. Metallurgical analysis indicates an iron production via the bloomery furnace technique. Analyzed samples show large slag inclusions (Fayalite, Wüstite, glass) within a mostly ferritic and pearlitic iron. The carbon contents varied between 0.2 wt% to around 0.8 wt%. ¹⁴C measurements on thermally extracted carbon give ¹⁴C ages between 2800 BP–3360 BP (calibrated ~1745 BC–900 BC). The reliability of the ¹⁴C measurements are discussed with respect to external (contamination during handling) and intrinsic contamination (e.g. fossil carbon sources during manufacture).

KEYWORDS: archaeometallurgy, iron swords, radiocarbon AMS dating, radiocarbon AMS dating of iron.

INTRODUCTION

Iron Mask Swords are somewhat mysterious iron objects. Recovered mostly from illegal diggings in the 1920s in the province of Luristan, Iran, the about 90 known objects (Muscarella 1989) are distributed in private and museum collections. Just recently one sword was recovered during a rescue excavation in Nurabad, Luristan, Iran (Hasanpur et al. 2015), with an inferred age (datum post quem) around 9th century BC.

All of the known swords are characterized by a disk-shaped pommel on the top of the handle with two mounted bearded heads on two sides, a rectangular shaped handle with two clamps and two kneeling animal figures on the lower part (see Figure 1). The blade is turned 90° with respect to the handle. The overall size of these objects is about 30–60 cm. They may well be the oldest complex iron objects known at present, but without knowing their age, this remains speculative.

Numerous attempts have been made to date these swords by indirect means (see e.g. Muscarella 1989), but lacking contextual finds, all these efforts are little more than educated guesses. Suggested ages range from 1100 BC–600 BC. A first experimental assessment of the age of these objects came from radiocarbon measurements on two Luristan swords from the Royal Ontario Museum and the Massachusetts Institute of Technology collection (2880 ± 60 BP and 2940 ± 60 BP, respectively; Cresswell 1992), placing them in the early part of the Iron Age. With respect to their homogeneity in style and structure, an overall short production period was assumed (Moorey 1991).

*Corresponding author. Email: mhuels@leibniz.uni-kiel.de.

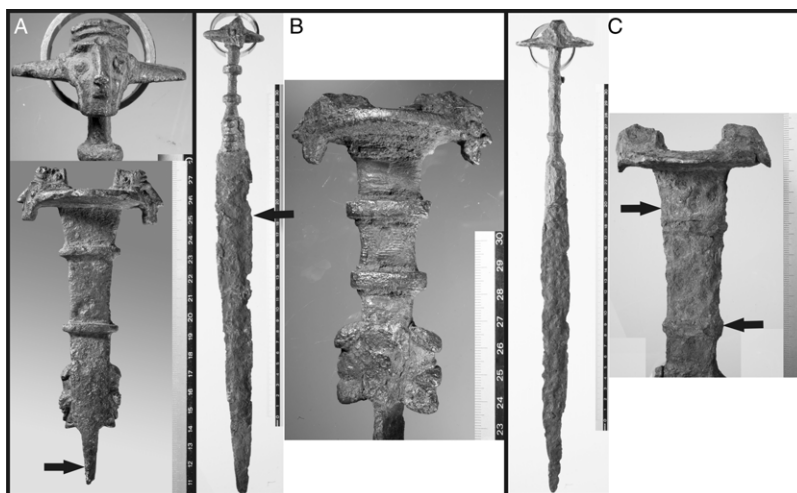


Figure 1 Iron Mask Swords for metallurgical analysis and ^{14}C measurement (A: IR-3743; B: IR-3745; C: IR-3746). Arrows mark the position for sampling for metallurgical and radiometric analyses. Photographs by Agnes Heitmann, Institute for Pre- and Protohistoric Archaeology, Christian-Albrechts-University Kiel, Germany.

In this study we present the results of metallurgical analysis and ^{14}C measurements for three Luristan swords, which were acquired recently by one of the authors (HF). After finishing our investigations, the swords were donated to the Royal Museums of Art & History, Brussels.

MATERIALS AND METHODS

Material

All three swords lack an archaeological context, which, in the beginning of our investigation, left open the possibility of a forgery. IR-3743 is a fragment of sword with a moderately well preserved hilt and the upper part of the blade, covered by corrosion with visible solid iron at the broken blade (Figure 1). The sword is sampled below the hilt on one side of the blade. IR-3745 and IR-3746 are complete swords, corroded with visible damages at the blades. The decoration-heads on the pommel are more corroded than on IR-3743. IR-3745 was sampled in the upper half of the blade, IR-3746 was sampled at the handle (two times from the opposite side). All samples are taken by using a cutting disk ($\sim 20\text{--}30 \times 5 \times 5$ mm).

Sample Preparation for Metallurgical Analysis

Iron samples IR-3743, IR-3745, and IR-3746 were embedded in PolyFast™ (Struers) with a SimpliMet™ XPS1 press (Buehler), grinded, polished, and etched with 3% Nital solution. After microstructure analysis of Nital etched cross sections, samples were polished again, etched with an Oberhoffer solution to reveal possible phosphorous (P) contents, followed by a second microstructure analysis of Oberhoffer etched cross sections. Microstructure analysis were done with reflecting light microscopy (MeF3A from the company Reichert-Jung). The carbon content was estimated by comparison with microstructures of known composition (Wever and Rose 1954; Rose and Hougardy 1972; Orlich and Rose 1973; Orlich and Pietrzeniuk 1976). Following microstructure analysis, mechanical properties such as micro-hardness were determined (Micro-hardness Micro-Duomat 4000E from the company Reichert-Jung with a force of 100P [20 s] and an increase of 40P/s). Finally, the

samples were inspected with SEM/EDX (Zeiss Gemini Ultra55plus, EDX-detector: Oxford X-act SD-detector. EHT: 5 kV, measuring time: 600,000 counts, calibration: standardless) for point analysis of the chemical composition of the metallurgic samples.

Sample Preparation for ¹⁴C Measurement

All surface areas from the different sword samples are thoroughly grinded using a corundum grinding tool, thereby removing the corrosion layer at the outside and possible surface-contaminated iron from the cutting process. Subsequently, smaller pieces are cut (length/width/thickness ~5/5/3 mm) with a metal cutter, again followed by a thorough grinding of shear surface areas. Finally, pieces are solvent cleaned using hot tetrahydrofuran, chloroform, ligroin, acetone, methanol, and water, using a computer-controlled “Soxhlet”-type series extractor (Bruhn et al. 2001). Carbon dioxide is released by closed-quartz-tube combustion with CuO (~5–6 times amount of sample weight) at 1000°C/24 hr (Cook et al. 2001; Hüls et al. 2004, 2011) and subsequent cryogenic purification of CO₂ (–70°C by dry-ice/ethanol slurry for removing H₂O, –130°C [frozen n-pentane] cool-trap to withhold SO₂ [Kusakabe 2005]).

AMS Measurements

The sample CO₂ was graphitized by the Bosch reaction with an iron catalyst (Vogel et al. 1984; Nadeau et al. 1998). The resulting mixture of graphite and iron powder was pressed into aluminum target holders for AMS ¹⁴C measurements with a 3MV HVEE Tandetron AMS system. ¹⁴C measurements are normalized to modern Oxalic Acid II standard (NBS SRM 4990C) and corrected for isotopic fractionation and background effects (Nadeau and Grootes 2013). ¹⁴C ages are translated to calendar ages using the software package OxCal4 (Ramsey and Lee 2013) and the IntCal13 dataset (Reimer et al. 2013).

RESULTS AND DISCUSSION

Metallurgy

Only a brief summary of the metallographic analyses is given here to provide the necessary details to evaluate and support the reliability of the ¹⁴C dates. A more comprehensive overview and discussion of the metallurgy will be given in a separate publication (Petri et al. in prep.).

The microscopic analysis of samples IR-3743, IR-3745, and IR3746 (see Figure 2) reveal in general two distinctive zonal structures with gradual transitions:

- IR-3743 (sampled on the upper part of the blade): Zone 1 contains a fine-grained ferritic structure with strings of cementite along grain boundaries (only detected in SEM/EDX), the estimated C-content is about ~0.02 wt%. Zone 1 contains small slag inclusions (Fayalite + Wüstite + Glass; more slag inclusions are observed in zone 1a). Zone 2 consists of a very fine-grained structure with mainly Ferrite, globular Pearlite, and Cementite along grain boundaries. This zone contains more slag inclusions. The C-content is estimated to between 0.1 and 0.5 wt%. The hardness ranges from about 100 mHV to about 200 mHV, whereas the hardness of zone 2 was higher than that of zone 1.
- IR-3745 (sampled at the blade): This sample shows a high content of very large slags (Fayalite + Wüstite + Glass). Within general ferritic grains of zone 1, Cementite needles are observed, particularly well developed in zone 1a. Overall, the C-content is low (~<0.02 wt%). Zone 2 consists of Ferrite and Pearlite, the Pearlite being partially globular. The carbon content varies between 0.02 and 0.1 wt%. The hardness ranges

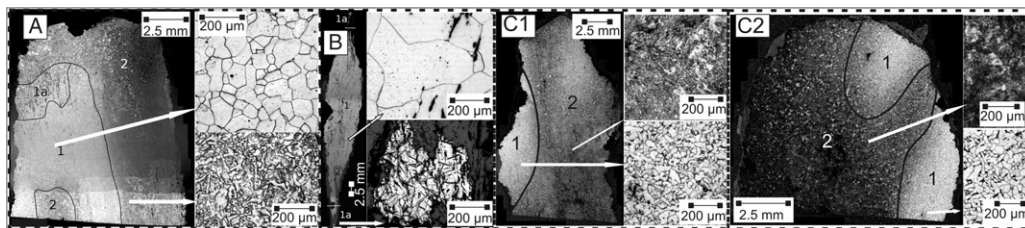


Figure 2 Microstructures of samples IR-3743 (A), IR-3745 (B), and IR-3746 (C1, C2) (Nital etched; left side pictures show whole metallographic sample, right side gives close-up). Numbers give structural zones (see description in text). Photographs by I. Petri, Institute for Pre- and Protohistoric Archaeology, Christian-Albrechts-University Kiel, Germany.

from about 100 mHV to about 185 mHV, while the hardness of zone 2 tends to be higher than that of zone 1. The inner part of the blade is softer than the outer part, but the highest hardness values are not measured at the cutting edges.

- IR-3746 (sampled at the handle): The sample shows two structural zones with no clear borders. Zone 1 contains a fine-grained ferritic-pearlitic Widmanstätten structure, the Pearlite being mostly globular. The slag content is relatively low, the slags are mostly fayalitic. The C-content raises continuously from about 0.1 wt% to the carbon content of zone 2. Zone 2 contains a fine-grained pearlitic structure, the Pearlite being mostly globular. Zone 2 shows some slag inclusions (Fayalite). The estimated C-content is about 0.7–0.8 wt%. The two metallurgical samples of this sword are comparably similar, even though being from the opposite ends of the handle. This indicates the manufacture of the handle from a rather homogenous single iron bloom. The hardness ranges from about 115 mHV to about 230 mHV, whereat the hardness of zone 2 was higher than that of zone 1.

For all samples no clear borders or linear structures such as bands of slag inclusions, oxidation horizons, or phosphorous enriched bands (“white lines”), characteristic for welding of different pieces, are observed. The zonal structures also do not show clear borders but gradual transitions into the next structure. As such, the structural zones appear original from an inhomogeneous iron bloom and are not caused by forge-welding of pieces of a different carbon content or by subsequent carburization of the finished object. The amount of slag inclusions and their composition indicates their origin from the bloomery process. Their elongated appearance and their orientation within the samples indicates subsequent hammering into form. The globular Pearlites show that the material has been intensively annealed over several hours. This is supported by the hardness measurements, even the areas with a C-content of about 0.7–0.8 wt% do not exceed a hardness of 230 mHV. As such, the intensive annealing was probably done to soften the material for subsequent fixing of the assembled different parts of the swords. For example, the outer part of the sample from sword IR-3743 shows traces of intensive cold working. Here the metal has been driven cold against the side of the animal figure that sits directly over the sample to clamp it into place.

The composition of the slag inclusions for the three sword samples by SEM-EDX analysis (see Table 1) give further insight into the production process. For example, the so-called G-value (Buchwald 2005), which is the ratio of (non-reduced) oxides coming from charcoal ashes, impurities of the used ore, and furnace construction material, divided by the oxides from the iron ore, gives information about the reduction grade of the ore during the iron smelting process. For the arbitrarily selected Luristan sword samples of this study, a gradual

Table 1 SEM-EDX measurements of slag inclusions (calculated averages from N single point measurements; n.d.: not detected).

	IR-3743 (N=16)	IR-3745 (N=10)	IR-3746-b (N=16)
CO ₂ wt%	6.0 ± 0.54	n.d.	13.7 ± 0
Na ₂ O wt%	0.4 ± 0.1	1.5 ± 0.2	0.5 ± 0
MgO wt%	2.8 ± 1.5	n.d.	2.7 ± 1.32
Al ₂ O ₃ wt%	6.2 ± 6.0	7.2 ± 7.1	7.6 ± 4.0
SiO ₂ wt%	27.0 ± 13.8	8.5 ± 8.9	32.7 ± 16.3
P ₂ O ₅ wt%	1.5 ± 0.6	5.1 ± 0.3	0.6 ± 0.1
SO ₃ wt%	4.4 ± 6.9	0.7 ± 0.1	n.d.
K ₂ O wt%	1.0 ± 1.2	2.5 ± 1.3	2.1 ± 1.3
CaO wt%	11.0 ± 5.3	4.4 ± 3.1	10.4 ± 3.5
TiO ₂ wt%	0.6 ± 0.0	n.d.	0.5 ± 0.1
MnO wt%	4.1 ± 3.9	n.d.	0.2 ± 0
FeO wt%	33.1 ± 29.5	70.0 ± 22.0	29.1 ± 27.8
MoO ₃ wt%	n.d.	n.d.	n.d.
BaO wt%	1.8 ± 2.1	n.d.	n.d.
G-value	52.0	18.8	76.4
$= (\text{CaO} + \text{Al}_2\text{O}_3 + \text{K}_2\text{O} + \text{MgO}) * 100 / (\text{FeO} + \text{MnO} + \text{BaO} + \text{P}_2\text{O}_5)$			

increase in G-values are observed, starting with a low value for IR-3745 (G=19), an intermediate value for IR-3743 (G=52) to a higher value for IR-3746 (G=76). Much higher values (>400) are observed for iron which is produced with the more advanced and efficient blast furnace technique (Buchwald 2005), developed during the late medieval period. The estimated low G-values between 19–76 are thus further proof for a production via the bloomery process, not to mention that the swords are genuine and not fakes. Admittedly, further and more detailed analysis with more samples would be needed for confirmation.

¹⁴C Measurements

The three Luristan swords IR-3743, -3745, and -3746, give ¹⁴C ages between 2800 BP and 3360 BP (see Table 2), calibrated to 1745 BC–900 BC (Figure 3). The oldest measured sword is IR-3745 with a low carbon content (<0.1 wt%C) and a low G-value. Samples IR-3743 and IR-3746 contain a higher carbon content (0.4 and 0.6 wt% C, resp.) and give ¹⁴C ages slightly older and younger, resp., than previously measured Luristan swords (Cresswell 1992). For both samples, the higher C-content allowed a duplicate carbon extraction and subsequent ¹⁴C measurements, which gave reproducible results. To test for possible fractionation effects occurring during graphitization and AMS-measurement of the small sample of IR-3745 (220 µg C measured), a comparable amount of CO₂ of sample IR-3746 (260 µg C) was graphitized and measured (see Table 2). The result is in agreement with the measurements done on normal sized samples (~1 mg C), indirectly supporting the ¹⁴C measurement of IR-3745.

Regarding the overall similarity of about 90 known Luristan swords (Muscarella 1989), a rather limited production period, between the 10th to 8th century BC, was suggested (e.g. Moorey 1991; Overlaet 2004), which is in contrast to the longer period suggested by our ¹⁴C dates. This raise the question to what extent ¹⁴C ages measured from extracted carbon from iron is reliable.

Table 2 Carbon yields and radiocarbon ages of samples IR-3743 (KIA51495), IR-3745 (KIA52135), and IR-3746 (KIA 52134).

Sample name	Lab ID	Sampled weight (mg)	Combusted weight (mg)	Carbon collected (mg)	Carbon measured (mg)	Carbon yield (wt%)	F ¹⁴ C (‰mC)	¹⁴ C age BP	δ ¹³ _(AMS) (‰VPDB)
IR-3743	KIA51495	2146.06	749.1	3.5	1.0	0.4 ± 0.1	68.03 ± 0.18	3095 ± 21	-21.90 ± 0.35
			707.1	2.4	2.1		67.83 ± 0.20	3118 ± 24	-20.79 ± 0.46
							Weighted average	3105 ± 16	
IR-3745	KIA52135	3122.8	1793.7	0.2	0.2	0.01	65.81 ± 0.30	3361 ± 37	-26.24 ± 0.39
IR.3746	KIA52134	6474.8	1097.6	6.3	1.0	0.6 ± 0.0	70.51 ± 0.25	2806 ± 29	-26.99 ± 0.19
			997.3	5.8	0.9		70.67 ± 0.23	2789 ± 26	-28.71 ± 0.13
							Weighted average	2797 ± 19	
			997.3	5.8	0.3		70.69 ± 0.30 ¹	2787 ± 35 ¹	-26.24 ± 0.39 ¹

¹Part of available sample CO₂ of IR-3746 has been reduced using a comparable small amount (~0.26 mg C) as was available for graphitization and AMS ¹⁴C measurement of sample IR 3745 to test possible fractionation effects in analyzing small samples.

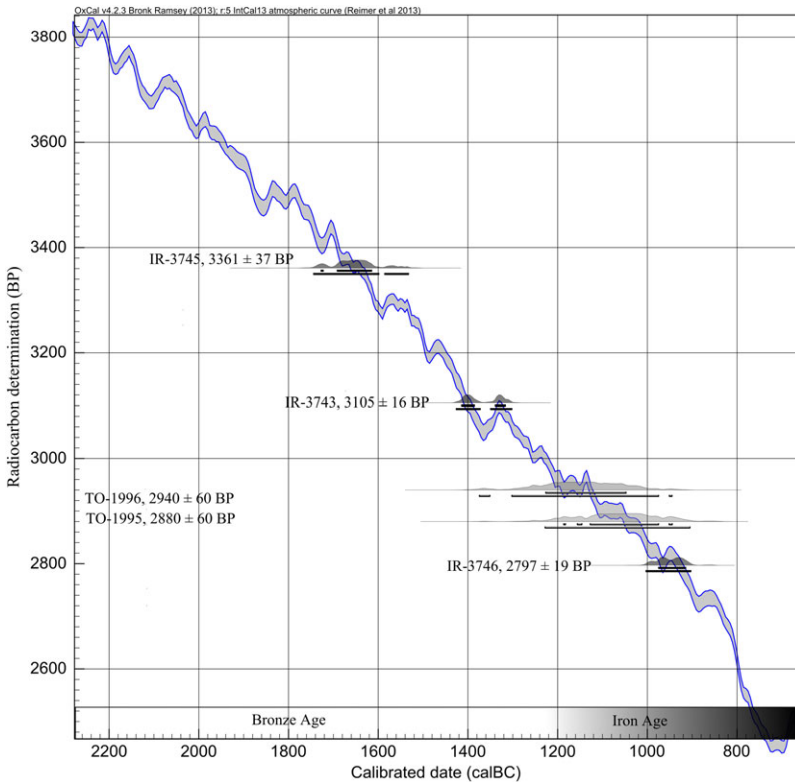


Figure 3 Calibrated sample ages of IR-3743, IR-3745, and IR-3746. For comparison, previously dated Luristan swords (Cresswell 1992) are shown in pale gray.

¹⁴C dating of iron in principle measures the age of dissolved carbon within the iron lattice, incorporated during the production of the iron. The main carbon source is coming from the fuel used for smelting the iron ore and for subsequent forging. A reasonable assumption for early metal production is that charcoal, made from almost contemporaneous trees, was used, which should give an age effect of only a few decades (Rehder 1991). For a local iron production site in Northern Germany from the 3rd century AD, anthracological analysis have indicated a wood age range up to a few decades (Dörfler and Wiethold 2000), which, although not directly applicable, lends further support for a small wood age effect. And indeed, for a number of studies regarding ¹⁴C dating of iron objects, a low wood age effect seems to have been indicated (e.g. Van der Merwe 1969; Cresswell 1992; Igaki et al. 1994; Nakamura 1995; Possnert and Wetterholm 1995; Cook et al. 2001; Scharf et al. 2004; Park et al. 2010; Hüls et al. 2011; Leroy et al. 2015).

Further carbon contamination sources could influence the carbon isotope composition during the production process, as was summarized by Craddock et al. (2002), namely the addition of fossil carbon, either coming from the use of fossil fuel sources (e.g. coke), or the use of calcite or lime as a flux ingredient (to increase the reduction efficiency and Fe yield from the ore), or coming from the geological material within the ore itself. The use of fossil fuel, such as pit-coal or coke, was introduced much later in iron technology, in the 11th century AD in China and the 17th century AD in Europe (Wikipedia 2018). If fossil fuel would have been

used here at any stage of the production process (smelting, smithing), the resulting ^{14}C age would become much older ($>>10,000$ years) as, for example, was shown by Park et al. (2008) and Craddock et al. (2002).

The use of calcite as a flux ingredient is more difficult to disprove. Using modern charcoal as fuel, roasted iron ore, and calcite as ingredients for a smelting experiment, Oinonen et al. (2009) studied the effect of the addition of calcite with respect to the ^{14}C concentrations of the resulting iron bloom. Measured Ca and ^{14}C concentration within the iron bloom confirm the incorporation and apparent mixture of modern (from the charcoal) and fossil carbon (from the calcite), with an inferred contamination of more than 20% (> 2000 years). Unfortunately, their data (e.g. measured calcium concentrations) cannot be compared directly with our data as they have made the measurements on bulk iron bloom samples.

CaO concentrations measured in the slag inclusions of our Luristan sword up to 11% (IR-3743) may also come from the ore used to make the iron. For example, the Apatite-Magnetite Deposit in central Iran (Esmailiy et al. 2016), would provide elements such as Al, Ca, K, and P, which become enriched during the smelting process within the slag inclusions. Depending on the pre-conditioning of the iron ore before smelting, e.g. roasting of the ore (Buchwald 2005), a significant portion of fossil carbon will get eliminated before the ore enters the smelting ovens. Indirect support for the reliability of ^{14}C dating of iron comes from the ^{14}C dating of some iron objects from the war booty of Nydam, Denmark, which are in good agreement with archaeological age estimates (Hüls et al. this issue), although elevated CaO concentrations up to 11 wt% were observed in some slag inclusions (Buchwald 2005).

Lacking hard evidence of a possible contribution from fossil carbon sources during the iron production of the three Luristan swords, we are inclined to accept our ^{14}C age estimates at this stage with, however, a larger uncertainty.

As was indicated by Scharf et al. (2004) and Hüls et al. (2011), the sampling of iron objects for ^{14}C measurements could potentially contaminate the overall extracted carbon due to the addition of fossil carbon from the modern steel tools used for cutting, which, however could be minimized by using larger iron pieces with a thorough surface cleaning. Recent ^{14}C measurements on experimentally produced modern iron (Hüls et al. 2011, 2019) and known archaeological iron from the early 1st millennium AD, seem to indicate that, instead of a previously assumed contamination by modern cutting tools, an intrinsic age offset, which is probably related to effects during the carbon uptake during the production process itself, may be possible, with a magnitude up to 100 years.

When applying an age offset of approximately 100 years to the measured ^{14}C ages of swords IR-3743, IR-3745, and IR-3746, the calibrated age range shifts to an indicated production period between 1650 BC and 800 BC, which is still a few centuries older than discussed by Moorey (1991) and Overlaet (2004).

CONCLUSIONS

For an arbitrary selection of three Luristan iron mask swords, metallurgical analysis and ^{14}C measurements have been performed. Earlier studies of these swords have indicated a mixture of a rather primitive iron production process and a sophisticated craftsmanship in the design of the decoration with a timing in the early Iron Age, around 1000 BC.

The microstructural analysis of the sword iron samples shows in general a heterogeneous mixture of low to intermediate carburized iron with a considerable slag content, indicative of a production via the bloomery process. Different to later iron objects, no clear signs of an intense forging process are observed, illustrating the early stage in iron making. The chemical composition of the slag inclusions seems to indicate an increase in the efficiency with respect to iron yield during the smelting process. Our ¹⁴C measurements indicate a comparatively long production period between 1650 BC and 800 BC, in contrast to earlier studies suggesting a short production period around 1000 BC. Further studies would be needed to gain more and detailed insight into the evolution of the early iron making during the transition of Bronze Age to the Iron Age.

ACKNOWLEDGMENTS

The authors are indebted to the Prof. Dr. Werner Petersen-Stiftung of Kiel, Germany, who financed part of this research. Thanks are also due to Profs. L. Kienle, R. Adelung, and the team of the Institute of Materials Science, CAU, Kiel, for letting us use their facilities. The competent help of Mrs. K Brandenburg, Mr. M.-D. Gerngroß, Mrs. Heitmann, Mr. K. Rath, Mrs. M. Schwitzke, and Mrs. Ch. Szillus is gratefully acknowledged. We appreciate the constructive comments given by two anonymous reviewers helping to shape the manuscript.

REFERENCES

- Bruhn F, Duhr A, Grootes PM, Mintrop A, Nadeau M-J. 2001. Chemical removal of conservation substances by “soxhlet”-type extraction. *Radiocarbon* 43(2A):229–237.
- Buchwald VF. 2005. Iron and steel in ancient times. Copenhagen: The Royal Danish Academy of Sciences and Letters.
- Cook AC, Wadsworth J, Southon JR. 2001. AMS radiocarbon dating of ancient iron artifacts: a new carbon extraction method in use at LLNL. *Radiocarbon* 43(2A):221–227.
- Craddock PT, Wayman ML, Jull AJ. 2002. The radiocarbon dating and authentication of iron artifacts. *Radiocarbon* 44(3):717–732.
- Cresswell RG. 1992. Radiocarbon dating of iron artifacts. *Radiocarbon* 34(3):898–905.
- Dörfler W, Wiethold J. 2000. Holzkohlen aus den Herdgruben von Rennfeueröfen und Siedlungsbefunden des spätkaiserzeitlichen Eisengewinnungs- und Siedlungsplatzes am Kammerberg bei Joldelund, Kr. Nordfriesland. In: Haffner A, Jöns H, Reichenstein J, editors. *Frühe Eisengewinnung in Joldelund, Kreis Nordfriesland: ein Beitrag zur Siedlungs- und Technikgeschichte Schleswig-Holsteins* / [aus dem Institut für Ur- und Frühgeschichte der Universität Kiel] (Universität). Bonn: Dr. Rudolf Habelt GmbH. p. 217–262.
- Esmailiy D, Zakizadeh S, Sepidbar F, Kanaanian A. 2016. The Shaytor apatite-magnetite deposit in the Kashmar-Kerman tectonic zone (central Iran): a Kiruna-type iron deposit. *Open Journal of Geology* 6(8):895–910.
- Hasanpur A, Hashemi Z, Overlaet B. 2015. The Baba Jilan graveyard near Nurabad, Pish-I Kuh, Luristan-A preliminary report. *Iranica Antiqua* 50:171–212.
- Hüls CM, Grootes PM, Nadeau M-J. 2011. Sampling iron for radiocarbon dating: influence of modern steel tools on ¹⁴C dating of ancient iron artifacts. *Radiocarbon* 53(1):151–160.
- Hüls CM, Grootes PM, Nadeau M-J, Bruhn F, Hasselberg P, Erlenkeuser H. 2004. AMS radiocarbon dating of iron artefacts. *Nuclear Instruments and Methods in Physics Research B* 223–224:709–715.
- Hüls CM, Meadows J, Rau A. 2019. Interpreting ¹⁴C measurements on 3rd–4th century AD iron artifacts from Nydam, Denmark. *Radiocarbon*. doi:10.1017/RDC.2019.15
- Igaki K, Nakamura T, Hirasawa M, Kato M, Sang M. 1994. Radiocarbon dating study of ancient iron artifacts with accelerator mass spectrometry. *Proceedings of the Japan Academy, Series B* 70(B):4–9.
- Kusakabe M. 2005. A closed pentane trap for separation of SO₂ from CO₂ for precise δ¹⁸O and δ³⁴S measurements. *Geochemical Journal* 39:285–287.
- Leroy S, L’Héritier M, Delqué-Kolic E, Dumoulin J-P, Moreau C, Dillmann P. 2015. Consolidation or initial design? Radiocarbon dating of ancient iron alloys sheds light on the reinforcements of French Gothic cathedrals. *Journal of Archaeological Science* 53:190–201.

- Moorey PRS. 1991. The decorated ironwork of the early Iron Age attributed to Luristan in western Iran. *IRAN* 29(May):1–12.
- Muscarella OW. 1989. Multi-piece iron swords from Luristan. In: De Meyer L, Haerincq E, editors. *Archaeologia Iranica et Orientalis miscellanea in honorem Louis Vanden Berghe*. Gent: Peeters Presse. p. 349–366.
- Nadeau M-J, Grootes PM. 2013. Calculation of the compounded uncertainty of ^{14}C AMS measurements. *Nuclear Instruments and Methods in Physics Research* 294:420–425.
- Nadeau M-J, Grootes PM, Schleicher M, Hasselberg P, Rieck A, Bitterling M. 1998. Sample throughput and data quality at the Leibniz-Labor AMS facility. *Radiocarbon* 40(1):239–245.
- Nakamura TH. 1995. AMS radiocarbon dating of ancient oriental iron artifacts at Nagoya University. *Radiocarbon* 37(2):629–636.
- Oinonen M, Haggren G, Kaskela A, Lavento M, Palonen V, Tikkanen P. 2009. Radiocarbon dating of iron: a northern contribution. *Radiocarbon* 51(2):873–881.
- Orlich J, Pietrzyk H-J. 1976. *Atlas zur Wärmebehandlung der Stähle Band 4*. Düsseldorf: Max-Planck-Institut für Eisenforschung. ISBN 3514001820. 282 p.
- Orlich J, Rose A. 1973. *Atlas zur Wärmebehandlung der Stähle Band 3*. Düsseldorf: Max-Planck-Institut für Eisenforschung. ISBN 3514001332. 264 p.
- Overlaet B. 2004. Luristan metalwork in the Iron Age. In: Stöllner T, Slotta R, Vatandoust A, editors. *Persiens Antike Pracht*. Bochum: Bergbau - Handwerk - Archäologie. p. 324–338.
- Park JS, Burr GS, Jull AJT. 2010. A thermal and acid treatment for carbon extraction from cast iron and its application to AMS dating of cast iron objects from ancient Korea. *Radiocarbon* 52(3):1312–1321.
- Park JS, Chunag A, Gelegdorj E. 2008. A technological transition in Mongolia evident in microstructure, chemical composition and radiocarbon age of cast iron artifacts. *Journal of Archaeological Science* 35(9):2465–2470.
- Possnert G, Wetterholm A. 1995. Radiocarbon dating of iron. *Norwegian Archaeological Review* 28(1):19–30.
- Ramsey CB, Lee S. 2013. Recent and planned developments of the program OxCal. *Radiocarbon* 55(2):720–730.
- Rehder JE. 1991. The decorated iron swords from Luristan: their material and manufacture. *IRAN* 29(May):13–19.
- Reimer PJ, Bard E, Bayliss A, Beck JW, Blackwell PG, Bronk Ramsey C, Buck C, Cheng H, Edwards RL, Friedrich M, Grootes PM, Guilderson TP, Haflidason H, Hajdas I, Hatté C, Heaton TJ, Hoffmann DL, Hogg AG, Hughen KA, Kaiser KF, Kromer B, Manning SW, Niu M, Reimer RW, Richards DA, Scott EM, Southon JR, Staff RA, Turney CSM, van der Plicht J. 2013. *IntCal13 and Marine13 radiocarbon age calibration curves 0–50,000 years cal BP*. *Radiocarbon* 55(4):1869–1887.
- Rose A, Hougardy H. 1972. *Atlas zur Wärmebehandlung der Stähle Band 2*. Düsseldorf: Max-Planck-Institut für Eisenforschung. ISBN 3514004137. 309 p.
- Scharf A, Kretschmer W, Morgenroth G, Uhl T, Kritzler K, Hunger K, Pernicka E. 2004. Radiocarbon dating of iron artifacts at the Erlangen AMS facility. *Radiocarbon* 46(1):175–180.
- Van der Merwe NJ. 1969. *The carbon-14 dating of iron*. Chicago: The University of Chicago Press.
- Vogel JS, Southon JR, Nelson DE, Brown TA. 1984. Performance of catalytically condensed carbon for use in accelerator mass spectrometry. *Nuclear Instruments and Methods in Physics Research* 5:289–293.
- Wever F, Rose A. 1954. *Atlas zur Wärmebehandlung der Stähle Band 1*. Berichtiger Nachdruck 1961. Düsseldorf: Max-Planck-Institut für Eisenforschung. Wikipedia. 2018. Coke (fuel). Available at: [https://en.wikipedia.org/wiki/Coke\(fuel\)](https://en.wikipedia.org/wiki/Coke(fuel)).